iMRI 2024;28(1):8-17
https://doi.org/10.13104/imri.2023.0027
eISSN 2384-1109

Original Article

Received: September 5, 2023
Revised: November 20, 2023
Accepted: December 6, 2023

Correspondence
Yong Eun Chung, MD
Department of Radiology,
Severance Hospital,
Yonsei University
College of Medicine,
50-1 Yonsei-ro, Seodaemun-gu,
Seoul 03722, Korea.
E-mail: yelv@yuhs.ac

Image Quality and Focal Lesion Detectability Analysis of Multiband Variable-Rate Selective Excitation Diffusion-Weighted Imaging of the Liver Using 3.0-T MRI

Ja Kyung Yoon[1], Yong Eun Chung[1], Jaeseung Shin[2], Eunju Kim[3], Nieun Seo[1], Jin-Young Choi[1], Mi-Suk Park[1], and Myeong-Jin Kim[1]

[1]Department of Radiology, Severance Hospital, Yonsei University College of Medicine, Seoul, Korea
[2]Department of Radiology, Samsung Medical Center, Seoul, Korea
[3]Clinical Science Leader, MR, Philips Healthcare, Seoul, Korea

Purpose: Acquisition time reduction in diffusion-weighted imaging (DWI) can be achieved by the combining multiband and variable-rate selective excitation (MB-VERSE). This study attempted to evaluate and compare the image quality (IQ) and focal lesion detectability of the respiratory-triggered MB-VERSE DWI with conventional DWI for liver magnetic resonance imaging.

Materials and Methods: The acquisition time, IQ, and focal lesion detectability of MB-VERSE DWI and conventional DWI were compared in 144 patients. Qualitative (overall IQ, IQ at the liver dome, sharpness of the liver margin, and degree of artifacts) and quantitative (signal-to-noise ratio [SNR], contrast-to-noise ratio [CNR], and apparent diffusion coefficient) IQ parameters were compared with the Wilcoxon signed-rank test. The diagnostic accuracy for focal lesion detectability was estimated with the mean figure of merit (FOM) from the area under the jackknife alternative free-response receiver operating characteristic curve.

Results: The MB-VERSE DWI exhibited significantly shorter scan time (153.1 ± 34.5 s vs. 225.1 ± 33.0 s, $p < 0.001$), poorer qualitative IQ (3.4 vs. 3.9, $p < 0.001$), lower SNR (34.4 vs. 50.0, $p < 0.001$), but comparable CNR (57.5 ± 49.0 vs. 78.9 ± 75.6, $p = 0.070$) compared to those of the conventional DWI. The MB-VERSE DWI exhibited similar per-lesion sensitivities (85.1%–88.1% vs. 88.1%–92.5%) and specificities (99.7%–99.8% vs. 99.5%–99.8%) of focal lesion detectability ($p > 0.050$) and similar diagnostic accuracy (FOM, 0.958 vs. 0.957, $p = 0.583$) compared to those of the conventional DWI.

Conclusion: MB-VERSE DWI exhibited a significantly shorter acquisition time than conventional DWI, with compromised overall IQ and lower SNR but preserved CNR and focal liver lesion detectability. MB-VERSE DWI may be a useful alternative for patients requiring a short acquisition time.

Keywords: Magnetic resonance imaging; Diffusion magnetic resonance imaging; Liver; Signal-to-noise ratio

This is an Open Access article distributed under the terms of the Creative Commons Attribution Non-Commercial License (http://creativecommons.org/licenses/by-nc/4.0/) which permits unrestricted non-commercial use, distribution, and reproduction in any medium, provided the original work is properly cited.

 Copyright © 2024 Korean Society of Magnetic Resonance in Medicine

INTRODUCTION

Diffusion-weighted imaging (DWI) is a useful technique for detecting and characterizing focal lesions in the liver and predicting the treatment response of hepatic tumors [1-3]. However, the long acquisition time of DWI is a drawback in the clinical setting. Multiband (MB) or simultaneous multislice (SMS) DWI offers reduced acquisition time via simultaneous excitation of multiple slices utilizing an MB pulse [4-6]. Indeed, the benefit of MB DWI in reducing the acquisition time without a significant compromise in image quality (IQ) was initially demonstrated in brain imaging [7]. Similar promising results have also been observed in hepatic and cardiac DWI [8,9]. However, the increase in MB acceleration factor is limited by the associated increase in noise, artifacts, and specific absorption rates [5,6].

The addition of a variable-rate selective excitation (VERSE) has been suggested to circumvent this problem. The VERSE pulse has been suggested for rapid magnetic resonance imaging (MRI) acquisition utilizing a time-varying gradient to optimize the radiofrequency pulse for a given peak B1 and excitation profile [4,10]. The resulting improvement in thick-slab profiles allows for more rapid imaging of limited volumes [10-13]. Recently, a combination of MB and VERSE (also known as multiband variable-rate selective excitation [MB-VERSE]) was hypothesized to decrease acquisition time with an acceptable overall IQ in body MRI [5,9]. However, the feasibility of MB-VERSE sequences in detecting focal lesions in the liver is yet to be elucidated.

Therefore, this study attempted to evaluate the qualitative and quantitative IQ and focal lesion detectability of the liver with respiratory-triggered MB-VERSE DWI compared to conventional DWI.

MATERIALS AND METHODS

This study was approved by the Institutional Review Board of Severance Hospital (4-2021-0861). The requirement for written informed consent was waived owing to the retrospective nature of the study. All work was conducted according to the 1964 Declaration of Helsinki.

Study Population

This retrospective study enrolled 152 patients who underwent liver or pancreaticobiliary MRI at our institution between October and December 2020. Excluding eight patients without MB-VERSE DWI, 144 patients with who underwent both MB-VERSE DWI and conventional DWI of the liver were eligible for final analysis (Fig. 1). Clinical data on patient age, sex, weight, height, and diagnosis were collected from electronic medical records.

MRI Acquisition

All examinations were performed utilizing a 3.0-T MRI unit (Ingenia CX; Philips Healthcare, Best, The Netherlands) equipped with a multichannel phased-array body coil. The MRI protocols differed according to the study; however, scanning parameters for conventional DWI and MB-VERSE DWI did not vary significantly (Supplementary Table 1). The conventional DWI was performed with the shortest repetition time (TR) (range, 2753.0–3890.4 ms), shortest echo time (TE) (range, 59.5–69.5 ms), three b-values (0, 50, and 800 s/mm^2) with number of excitation (NEX) of 4, and a sensitivity encoding (SENSE) factor of 2. The MB-VERSE DWI was performed with the shortest TR (range,

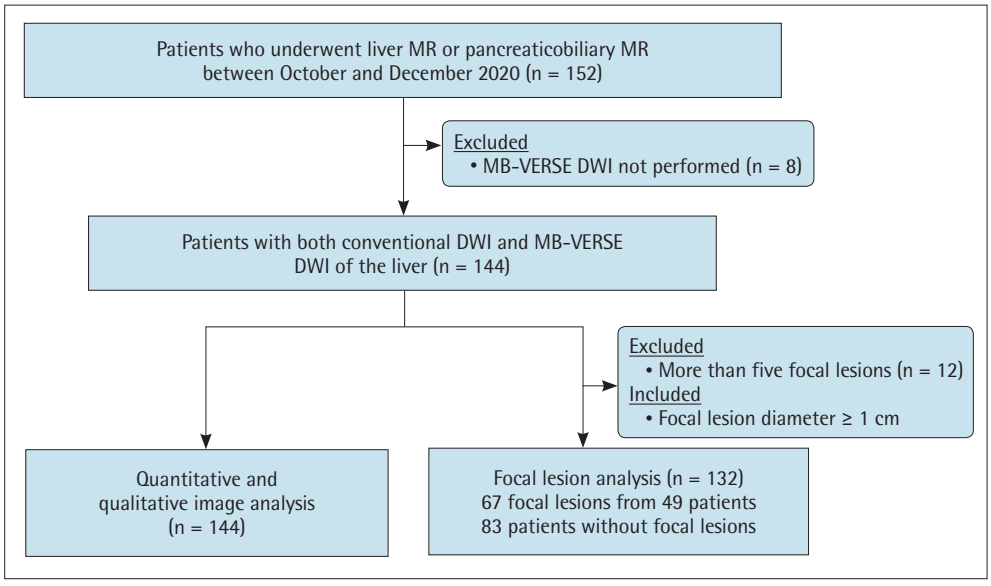

Fig. 1. Flowchart of study population and focal lesion analysis. MR, magnetic resonance; MB-VERSE, multiband variable-rate selective excitation; DWI, diffusion-weighted imaging.

1450.8–1837.7 ms), shortest TE (range, 61.7–79.6 ms), three b-values (0, 100, and 800 s/mm^2) and an MB factor of 2. The NEX for b-factors of 0 and 100 s/mm^2 was 2, while that for the NEX for b = 800 s/mm^2 was 8, to achieve a relative gain in SNR. Other scanning parameters were identical for both DWI scans: field of view, 40 × 40 cm; matrix size, 128 × 128; slice thickness, 5 mm; interslice gap, 1 mm; in-plane resolution, 3.125 × 3.125 mm^2. Both DWI sequences were performed with respiratory triggering. The MB-VERSE DWI protocol was set up by a physicist from the vendor, who was not directly involved in data manipulation and analysis. Routine MRI examinations comprised pre-contrast T2-weighted and dual-echo T1-weighted images, with or without dynamic contrast-enhanced T1-weighted images. For dynamic contrast-enhanced T1-weighted images, the arterial phase (30–35 s), portal phase (60 s), late phase (3 min), and delayed or hepatobiliary phase (20 min) were obtained with a fat-suppressed T1-weighted three-dimensional spoiled gradient echo sequence.

Quantitative Image Analysis

All scans were reviewed and analyzed by a baseline researcher (JKY, with 2 years of experience in abdominal imaging). All quantitative image analyses were performed on high b-value images (b = 800 s/mm^2) of both MB-VERSE DWI and conventional DWI scans. The quantitative IQ parameters included the signal-to-noise ratio (SNR), contrast-to-noise ratio (CNR), and apparent diffusion coefficient (ADC) value of the background liver parenchyma. Region of interest (ROI) with a mean size of 86.9 mm^2 (standard deviation [SD], 22.8 mm^2) were drawn at the corresponding area in the liver in both MB-VERSE DWI and conventional DWI scans to obtain the signal intensity of the liver (SI_{liver}), avoiding major vessels or artifacts. Identical ROIs were drawn at the corresponding areas in the liver on the ADC images of both sequences to obtain the ADC values of the background liver parenchyma. The SD of the noise signal intensity (SD_{noise}) was obtained by drawing an ROI in the same area just outside the body wall. The SNR was calculated by dividing the SI_{liver} by SD_{noise} (SI_{liver}/SD_{noise}) [14]. The CNR was calculated by dividing the difference between SI_{lesion} and SI_{liver} by SD_{noise} ([SI_{lesion}-SI_{liver}]/SD_{noise}), where SI_{lesion} was obtained by drawing the largest possible ROI of the focal liver lesion [14].

Qualitative Image Analysis

Two readers (YEC and JS, with 15 and 2 years of experience in abdominal imaging, respectively) independently reviewed the high b-value images of conventional DWI and MB-VERSE DWI in random order. The readers were blinded to the DWI sequences, patient histories, and clinical diagnoses. The IQ parameters included overall IQ, IQ at the liver dome (both right and left), sharpness of the liver margin, and degree of artifacts (i.e., motion artifacts, susceptibility artifacts, and B0 inhomogeneities). IQ at the liver dome was evaluated separately to

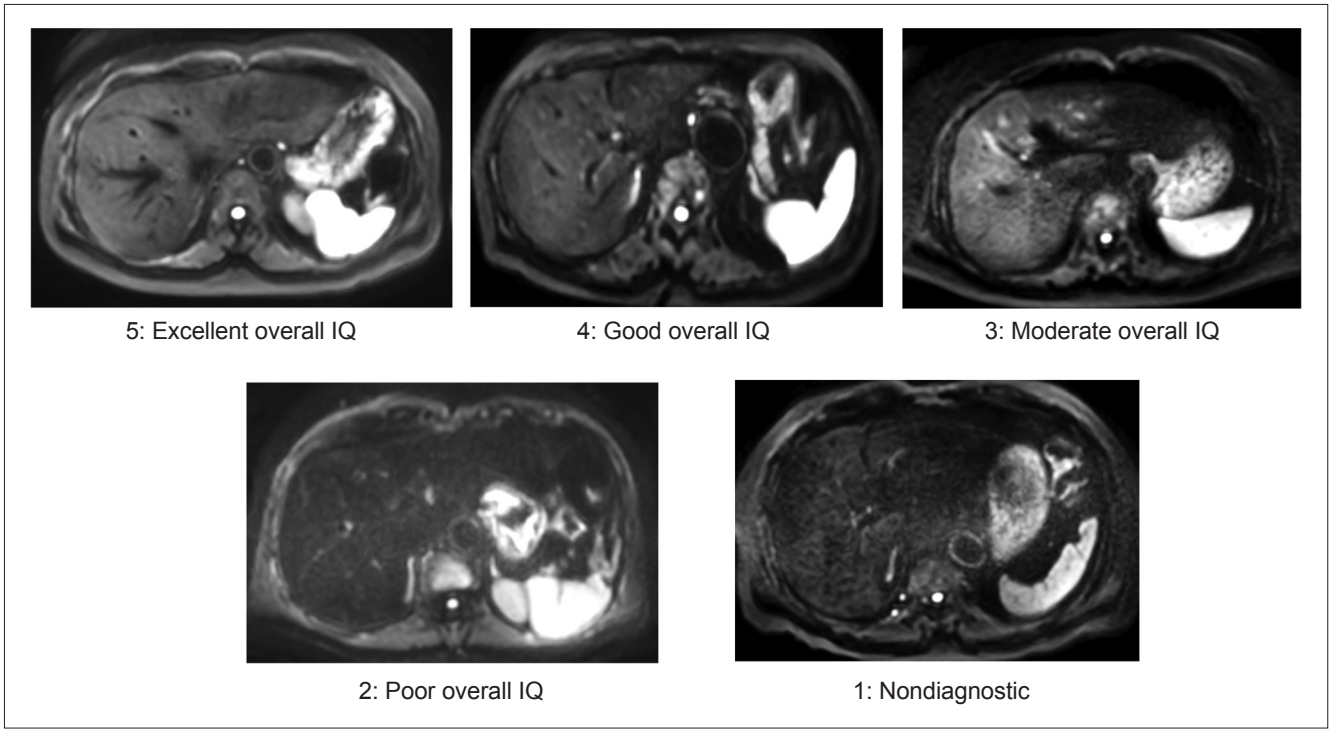

Fig. 2. Scores for overall IQ evaluation. Qualitative evaluation of overall IQ was evaluated on a five-point scale, five being excellent overall IQ (sharp liver margin and none or minimal artifact) to non-diagnostic IQ (severe blurring of liver margin with severe artifact). IQ, image quality.

account for more severe susceptibility artifacts due to the lung-liver border and pulsation artifacts [15,16]. The two readers evaluated IQ parameters on a five-point scale. The overall IQ and IQ at the liver dome were scored as follows: 5, excellent with sharp liver margin and minimal artifacts; 4, good; 3, moderate; 2, poor; and 1, non-diagnostic with severely blurred liver margin and severe artifacts (Fig. 2). The sharpness of the liver margin was scored as follows: 5, sharp liver margin; 4, mild blurring of the liver margin; 3, moderate blurring of the liver margin; 2, severe blurring of the liver margin; and 1, non-diagnostic. The degree of artifacts was scored as follows: 5, no artifacts; 4, mild artifacts, without affecting interpretation; 3, moderate artifacts, potentially affecting interpretation; 2, severe artifacts, definitely affecting interpretation; and 1, extensive artifacts yielding non-diagnostic images. The average score of the readers was considered as the final score for each conventional DWI and MB-VERSE DWI scan.

Focal Lesion Analysis

The baseline researcher identified focal liver lesions with high signal intensity on the high b-value image (b = 800 s/mm^2) on conventional DWI with reference to other sequences, including T2 and T1 dynamic contrast enhancement studies. The diagnosis of focal lesions was established based on typical imaging findings (e.g., hepatocellular carcinoma [HCC] with typical imaging features) [17], stability on imaging studies for at least one year before or after the studied scans, or histopathology. Studies with more than five focal lesions with positive diffusion restriction (n = 12) were excluded because of the potential confounding effects of multiple lesions [18]. Lesions smaller than 1 cm on the high b-value conventional DWI were excluded because of the low resolution of DWI [19]. Finally, 67 focal lesions ≥ 1 cm from 49 patients were identified. For the free-response analysis, a total of 132 scans (49 scans with focal lesions and 83 scans without focal lesions) were included.

The two readers performed focal lesion detectability analyses at least 2 weeks after qualitative image analysis. The 132 scans were reviewed randomly, with the readers unaware of the presence or absence of focal lesions. The readers independently identified up to five focal liver lesions (≥ 1 cm) each on high b-value images of conventional DWI and MB-VERSE DWI. Two readers recorded the size, segment location, and the image number of the focal lesions. Lesion conspicuity and detectability scores for each lesion on conventional DWI and MB-VERSE DWI were also recorded. The conspicuity score was assessed on a five-point scale as follows: 5, very well-delineated and sharply defined; 4, well-delineated; 3, moderately conspicuous; 2, fairly conspicuous; and 1, barely delineated (Fig. 3). The focal lesion detectability score was assessed as follows: 5, definitely present focal liver lesion; 4, probably present

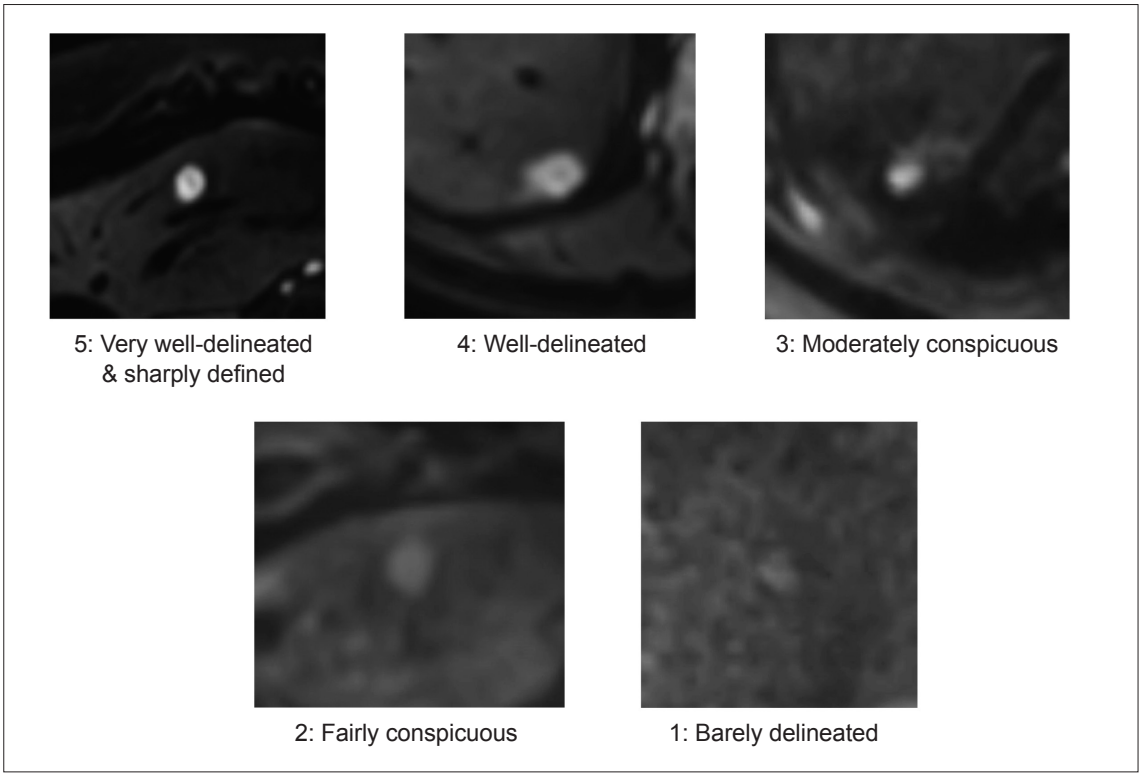

Fig. 3. Scores for focal lesion conspicuity. Qualitative evaluation of focal lesion conspicuity was evaluated on a five-point scale.

focal liver lesion; 3, equivocal focal liver lesion; 2, probably no focal liver lesion; and 1, definitely no focal liver lesion. A lesion was considered detected when the mean detectability scores of the two readers were ≥ 3 points, whereas lower mean scores were considered not detected. For the per-patient analysis, the readers attempted to correctly identify whether the patients had focal liver lesions.

Statistical Analysis

Statistical analyses were performed using commercially available software. Most analyses were performed with R version 4.0.4 (The R Foundation for Statistical Computing, Vienna, Austria). The mean values of the quantitative IQ parameters were compared with the Wilcoxon signed-rank test. The mean scores of the qualitative IQ parameters from the two readers were also compared utilizing the Wilcoxon signed-rank test.

For the focal lesion analysis, the focal lesion conspicuity and detectability scores of the two readers were averaged and compared utilizing the Wilcoxon signed-rank test. The performances of conventional DWI and MB-VERSE DWI per-patient and per-lesion detectability for each reader were analyzed with SAS (version 9.4; SAS Inc., Cary, NC, USA). The jackknife alternative free-response receiver operating characteristic (JAFROC) method was utilized to analyze and compare the performance of conventional DWI and MB-VERSE DWI for focal lesion detection. Mean diagnostic accuracy was calculated according to the mean figure of merit (FOM, θ) from the area under the JAFROC curve [20,21]. The JAFROC FOMs for comparing the detectability of conventional DWI and MB-VERSE DWI were evaluated using random readers and random cases method.

Inter-reader agreement on the scoring of the overall IQ, IQ at the liver dome, sharpness of the liver margin, degree of artifacts, focal lesion conspicuity, and detectability was compared using weighted kappa [22]. Kappa coefficients (κ) indicated the degree of agreement as follows: 0.81–1.00, excellent; 0.61–0.80, substantial; 0.41–0.60, moderate; 0.21–0.40, fair; and 0.00–0.20, poor [23]. Results with p-values < 0.05 were considered statistically significant.

Table 1. Baseline patient demographics and focal liver lesion characteristics

Characteristics	Values
Patient characteristics (n = 144)	
Male	86 (59.7)
Age (yr)	60.4 ± 12.5
BMI (kg/m^2)	24.1 ± 3.1
Background liver disease	
None	66 (45.8)
Chronic hepatitis B	50 (34.7)
Chronic hepatitis C	4 (2.8)
NAFLD	10 (41.7)
Alcoholic liver disease	4 (16.7)
Chronic liver disease, unknown etiology	10 (41.7)
Reason for study	
HCC surveillance or hepatic nodule characterization	55 (38.2)
Follow-up of HCC or cholangiocarcinoma	35 (24.3)
Benign pancreaticobiliary disease	11 (7.6)
Metastasis evaluation	43 (29.9)
Focal lesion characteristics	67 lesions in 49 patients
Size (cm)	1.6 (1.1–12.2)
Number of patients with focal lesions (n = 49)	
1	38 (26.4)
2	7 (4.9)
3	1 (0.7)
4	3 (2.1)
5	0 (0.0)
Diagnosis of focal lesions (n = 67)	
HCC or cholangiocarcinoma	23 (34.3)
Metastasis from extrahepatic malignancy	19 (28.4)
Benign	25 (37.3)

Data are presented as numbers (%), mean ± standard deviation, or the median (1st quartile, 3rd quartile).
BMI, body mass index; NAFLD, non-alcoholic fatty liver disease; HCC, hepatocellular carcinoma.

RESULTS

Baseline Patient Demographics

The baseline patient characteristics are presented in Table 1. This study included 86 males and 58 females. The reasons for undergoing MRI included surveillance for HCC or hepatic nodule characterization (n = 55, 38.2%), follow-up for HCC (n = 35, 24.3%), evaluation of benign pancreaticobiliary disease (n = 11, 7.6%), and evaluation of metastasis of extrahepatic malignancies (n = 43, 29.9%). Extrahepatic malignancies included primary malignancies such as colorectal (n = 17), pancreaticobiliary (n = 10), stomach (n = 4), breast (n = 4), choroidal melanoma (n = 4), lung (n = 1), ovary (n = 1), kidney (n = 1), and thyroid cancer (n = 1).

MRI Acquisition Time of Conventional DWI and MB-VERSE DWI

The MB-VERSE DWI demonstrated a 32.0% reduction in mean acquisition time compared with conventional DWI (mean ± SD, 153.1 ± 34.5 s vs. 225.1 ± 33.0 s, p < 0.001). The mean TR of MB-VERSE DWI was significantly lower than that of the conventional DWI (1609.0 ± 83.3 ms vs. 3226.4 ± 200.1 ms, p <

Table 2. Comparison of quantitative and qualitative IQ parameters between conventional DWI and MB-VERSE DWI

	Conventional DWI		MB-VERSE DWI		p*
	Meam ± SD	κ	Meam ± SD	κ	
Quantitative parameters					
SNR	50.0 ± 34.2	-	34.4 ± 30.1	-	< 0.001
CNR	78.9 ± 75.6	-	57.5 ± 49.0	-	0.070
ADC value, $\times 10^{-3}$ s/mm^2	1.2 ± 0.2	-	1.0 ± 0.3	-	0.012
Qualitative parameters					
Overall IQ	3.9 ± 0.6	0.412	3.4 ± 0.7	0.358	< 0.001
IQ at the liver dome	4.2 ± 0.5	0.221	3.4 ± 0.9	0.433	< 0.001
Sharpness of the liver margin	4.0 ± 0.5	0.313	3.9 ± 0.7	0.379	0.033
Degree of artifact	3.8 ± 0.5	0.215	3.3 ± 0.7	0.330	< 0.001

*Wilcoxon signed-rank test was utilized.
IQ, image quality; DWI, diffusion-weighted imaging; MB-VERSE, multiband variable-rate selective excitation; SNR, signal-to-noise ratio; CNR, contrast-to-noise ratio; ADC, apparent diffusion coefficient; κ, weighted kappa.

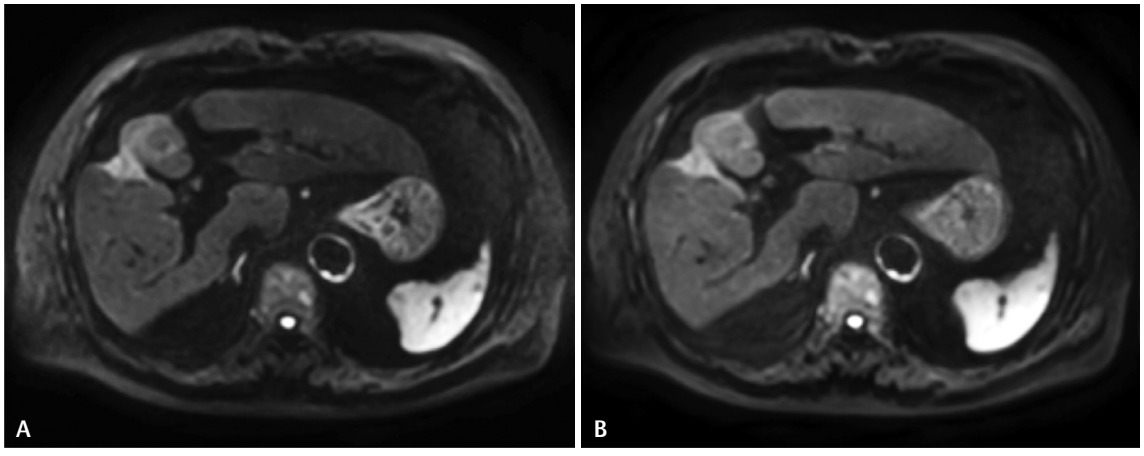

Fig. 4. Representative high b-value images (b = 800 s/mm^2) of conventional DWI and MB-VERSE DWI. DWI scans of 80-year-old male patient with history of HCC and underlying liver cirrhosis. Qualitative IQ was good for MB-VERSE DWI (average score of 4) (A) and excellent for conventional DWI (average score of 4.5) (B). MB-VERSE DWI exhibited lower SNR than the conventional DWI (25.4 vs. 102.5) but with shorter acquisition time (125.1 s vs. 226.9 s). DWI, diffusion-weighted imaging; MB-VERSE, multiband variable-rate selective excitation; SD, standard deviation; HCC, hepatocellular carcinoma; IQ, image quality; SNR, signal-to-noise ratio.

Table 3. Focal lesion detectability on conventional DWI and MB-VERSE DWI

	Conventional DWI	MB-VERSE DWI	p
Reader 1			
Sensitivity per lesion	88.1 (80.3, 95.8)	85.1 (76.5, 93.6)	0.151
Specificity per lesion	99.8 (99.5, 100.0)	99.8 (99.5, 100.0)	> 0.999
Sensitivity per patient	93.6 (86.6, 100.0)	91.5 (83.5, 99.5)	0.312
Specificity per patient	97.7 (94.4, 100.0)	97.7 (94.4, 100.0)	> 0.999
Reader 2			
Sensitivity per lesion	92.5 (86.2, 98.8)	88.1 (80.3, 95.8)	0.076
Specificity per lesion	99.5 (98.9, 100.0)	99.7 (99.2, 100.0)	0.317
Sensitivity per patient	95.7 (90.0, 100.0)	93.6 (86.6, 100.0)	0.312
Specificity per patient	96.5 (92.6, 100.0)	97.7 (94.4, 100.0)	0.314

Data are presented as percentages (95% confidence intervals).
DWI, diffusion-weighted imaging; MB-VERSE, multiband variable-rate selective excitation.

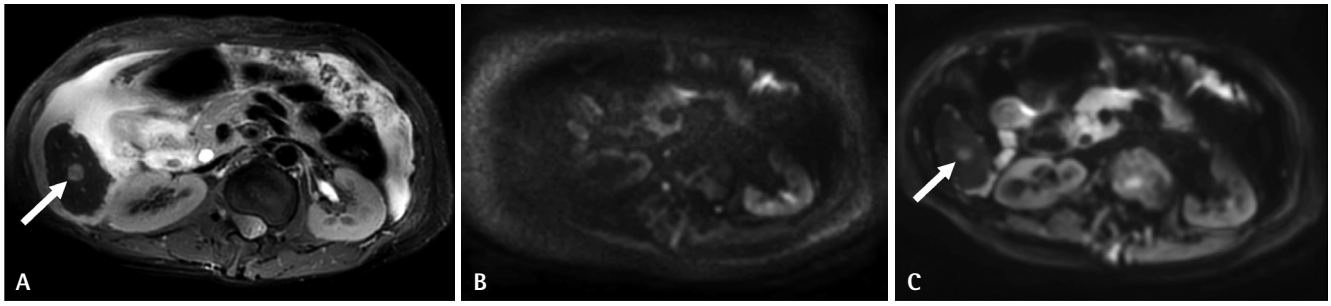

Fig. 5. Focal lesions on high b-value images (b = 800 s/mm^2) of conventional DWI and MB-VERSE DWI. DWI scans of 59-year-old female patient with colon cancer patient. A focal liver lesion with moderately high signal intensity was noted on T2-weighted image (A) and conventional DWI (arrow) (C). This lesion was not visualized on the MB-VERSE DWI owing to poor IQ and severe degree of artifacts. Both readers scored the lesion as barely delineated on the MB-VERSE DWI (conspicuity score of 1) and moderately conspicuous on the conventional DWI (conspicuity score of 3). The MB-VERSE DWI exhibited lower qualitative IQ and SNR (average scores of 4 and 47.5, respectively) than those of the conventional DWI (average scores of 2 and 29.2, respectively). DWI, diffusion-weighted imaging; MB-VERSE, multiband variable-rate selective excitation; IQ, image quality; SNR, signal-to-noise ratio.

0.001). The mean TE of MB-VERSE DWI was significantly longer than that of the conventional DWI (66.4 ± 2.2 ms vs. 60.8 ± 2.6 ms, p < 0.001).

Quantitative IQ Analysis

A comparison of the quantitative IQ parameters between MB-VERSE DWI and conventional DWI is presented in Table 2. MB-VERSE DWI exhibited a 15.6% decrease in SNR compared with the conventional DWI (34.4 vs. 50.0, p < 0.001). However, the CNRs of MB-VERSE DWI and conventional DWI were not significantly different (57.5 vs. 78.9, p = 0.070). The ADC values of the liver parenchyma were significantly lower on MB-VERSE DWI than on conventional DWI (1.0 vs. 1.2, p = 0.012).

Qualitative IQ Analysis

A comparison of the qualitative IQ parameters between MB-VERSE DWI and conventional DWI is presented in Table 2. The MB-VERSE DWI exhibited significantly lower overall IQ (3.4 vs. 3.9, p < 0.001), sharpness of the liver margin (3.9 vs. 4.0, p = 0.033), and IQ at liver dome (3.4 vs. 4.2, p < 0.001) than conventional DWI (Table 2, Fig. 4). The degree of artifacts was significantly more prominent on MB-VERSE DWI than on the conventional DWI (3.3 vs 3.8, p < 0.001). The inter-reader agreements for the overall IQ, sharpness of the liver margin, IQ at the liver dome, and degree of artifacts on conventional DWI and MB-VERSE DWI were fair to moderate.

Focal Lesion Analysis

The characteristics of the focal lesion are presented on Table 1. Among the 67 focal lesions, 23 (34.3%) were HCCs or cholangiocarcinomas, and 19 (28.4%) were metastases from extrahepatic malignancies, including colorectal cancer (n = 12), pancreaticobiliary cancer (n = 4), lung cancer (n = 2), and ovarian cancer (n = 1). The remaining 25 focal lesions were benign, including hepatic cysts (n = 13), hepatic hemangiomas (n = 8), inflammatory lesions (n = 3), and a hepatic adenoma (n = 1). Eight lesions (11.9%) were pathologically diagnosed, whereas 59 (88.1%) lesions were diagnosed based on typical imaging features or stability for at least one year.

Table 4. The FOM of the JAFROC analysis of per-lesion focal lesion detectability on conventional DWI and MB-VERSE DWI

	Conventional DWI	MB-VERSE DWI	p
Reader 1	0.957 (0.918, 0.997)	0.957 (0.917, 0.997)	0.520
Reader 2	0.956 (0.916, 0.996)	0.960 (0.921, 0.999)	0.347
Average	0.957 (0.947, 0.966)	0.958 (0.941, 0.976)	0.583

Data are presented as FOMs (95% confidence intervals).
FOM, figure of merit; JAFROC, jackknife alternative free-response receiver operating characteristic; DWI, diffusion-weighted imaging; MB-VERSE, multiband variable-rate selective excitation.

Focal lesions were significantly less conspicuous in the MB-VERSE DWI than in the conventional DWI (3.6 ± 1.4 vs. 3.6 ± 1.1, p = 0.032). However, the per-lesion and per-patient sensitivities and specificities of MB-VERSE DWI were not significantly different from those of conventional DWI (p > 0.05) (Table 3). Only two focal lesions were correctly detected on conventional DWI but not visualized on the MB-VERSE DWI because of poor IQ and severe artifacts (Fig. 5). The per-lesion FOMs from the JAFROC analysis of MB-VERSE DWI and conventional DWI for each reader are presented in Table 4. The reader-averaged FOMs determined with the mean value of the JAFROC analysis were not significantly different between MB-VERSE DWI and conventional DWI (0.958 vs. 0.957, p = 0.583).

Focal lesion conspicuity exhibited moderate (κ = 0.413) and fair (κ = 0.319) inter-reader agreement on conventional DWI and MB-VERSE DWI, respectively. Focal lesion detectability exhibited fair (κ = 0.401) and substantial (κ = 0.610) inter-reader agreement on conventional DWI and MB-VERSE DWI, respectively.

DISCUSSION

This study demonstrated that respiratory-triggered MB-VERSE DWI significantly reduced the acquisition time by 32.0%, with an expected compromise in overall IQ. Despite the trade-off in IQ, the CNR and lesion detectability of focal liver lesions on MB-VERSE DWI were not significantly different from those on conventional DWI.

MB-VERSE DWI significantly decreased the acquisition time at the expense of qualitative and quantitative IQ parameters compared with conventional DWI. This finding is comparable to previous studies that demonstrated a decrease in signal intensity or SNR in MB or SMS DWI compared with conventional DWI [24,25]. However, the CNR was not significantly compromised, possibly because the increase in contrast overrode the increase in noise [25]. Focal lesion detectability was also comparable between MB-VERSE DWI and conventional DWI which was similar to previous studies in which the detection rates of focal liver lesions and pelvic lymph nodes did not significantly decrease with MB DWI [24,25]. Hence, MB-VERSE DWI may be a useful alternative when a short acquisition time is crucial (e.g., in patients with claustrophobia or back pain, or in pediatric or elderly patients).

Consistent with previous reports, the ADC values of the liver parenchyma on MB-VERSE DWI were significantly lower than those on conventional DWI but within the range reported in the literature [24,26,27]. Lower ADC values may be associated with shorter TR, consistent with previous reports on MB DWI [24,28,29]. The shortened TR may result in incomplete recovery of the longitudinal magnetization and signal saturation (or the T1 saturation effect), leading to signal saturation in b = 0 s/mm^2 images. However, the T1 saturation effect was mitigated or negligible at b = 800 s/mm^2 because the longitudinal magnetization reached a steady state (owing to a later scanning time point) [29]. This discrepancy in the T1 saturation effect may explain the significantly lower ADC values in the liver parenchyma on MB-VERSE DWI than on conventional DWI. In addition, the lower SNR may be attributed to the lower ADC values in MB-VERSE DWI [28].

This study had some limitations. First, the retrospective study design has an inherent selection bias. Second, variations in MRI parameters may have affected the IQ, focal lesion conspicuity, and focal lesion detectability. Indeed, the b-values for conventional DWI and MB-VERSE DWI differed, which may have affected the ADC values of the liver parenchyma in each sequence. Third, no further acceleration beyond an MB factor of two was evaluated. However, we believe an MB acceleration factor of two may produce a balance between acquisition time reduction, SNR, and focal lesion detectability, based on previous reports suggesting a compromise between IQ and diagnostic performance in MB factors greater than 2 [25,26,30,31]. Fourth, only a few focal lesions were pathologically diagnosed. With the aim of focal lesion detection rather than diagnosis, a non-invasive diagnosis of focal lesions utilizing typical imaging findings or stability for at least one year seems sufficient. Finally, the inter-reader agreements for IQ, focal lesion conspicuity, and focal lesion detectability were fair to substantial, although within the range of kappa values reported in previous studies on the IQ of MB DWI [24,26,30,31].

In conclusion, MB-VERSE DWI significantly reduced the acquisition time with compromised quantitative and qualitative IQ but with comparable CNR and preserved focal lesion detectability. Further optimization of the MB-VERSE DWI technique may help improve IQ with a shorter acquisition time.

Supplementary Materials

The online-only Data Supplement is available with this article at https://doi.org/10.13104/imri.2023.0027.

Availability of Data and Material

The datasets generated or analyzed during the study are available from the corresponding author on reasonable request.

Conflicts of Interest

Yong Eun Chung who is on the editorial board of the *Investigative Magnetic Resonance Imaging* was not involved in the editorial evaluation or decision to publish this article. Eunju Kim is an employee at *Philips Healthcare Korea*, but was not directly involved in the research data. All remaining authors have no competing interests to declare that are relevant to the content of this article.

Author Contributions

Conceptualization: Ja Kyung Yoon, Yong Eun Chung. Data curation: all authors. Formal analysis: Ja Kyung Yoon. Investigation: Ja Kyung Yoon, Yong Eun Chung. Methodology: Ja Kyung Yoon, Yong Eun Chung, Jaeseung Shin, Eunju Kim. Project administration: Yong Eun Chung. Resources: Ja Kyung Yoon, Yong Eun Chung, Eunju Kim. Supervision: Yong Eun Chung. Validation: Ja Kyung Yoon, Yong Eun Chung, Jaeseung Shin. Visualization: Ja Kyung Yoon. Writing—original draft: Ja Kyung Yoon, Yong Eun Chung. Writing—review & editing: all authors.

ORCID iDs

Ja Kyung Yoon	https://orcid.org/0000-0002-3783-977X
Yong Eun Chung	https://orcid.org/0000-0003-0811-9578
Jaeseung Shin	https://orcid.org/0000-0002-6755-4732
Eunju Kim	https://orcid.org/0000-0002-9718-1156
Nieun Seo	https://orcid.org/0000-0001-8745-6454
Jin-Young Choi	https://orcid.org/0000-0002-9025-6274
Mi-Suk Park	https://orcid.org/0000-0001-5817-2444
Myeong-Jin Kim	https://orcid.org/0000-0001-7949-5402

Funding Statement
None

Acknowledgments
None

REFERENCES

1. Taouli B, Koh DM. Diffusion-weighted MR imaging of the liver. Radiology 2010;254:47-66.
2. Bae H, Lee SA, Choi JW, Hwang SH, Park S, Park MS. Effectiveness of hepatocellular carcinoma surveillance and an optimal surveillance interval: nationwide cohort of Korea. Yonsei Med J 2021; 62:758-766.
3. Lee JS, Chon YE, Kim BK, et al. Prognostic value of alpha-fetoprotein in patients who achieve a complete response to transarterial chemoembolization for hepatocellular carcinoma. Yonsei Med J 2021;62:12-20.
4. Hargreaves BA, Cunningham CH, Nishimura DG, Conolly SM. Variable-rate selective excitation for rapid MRI sequences. Magn Reson Med 2004;52:590-597.
5. Barth M, Breuer F, Koopmans PJ, Norris DG, Poser BA. Simultaneous multislice (SMS) imaging techniques. Magn Reson Med 2016; 75:63-81.
6. Yoon JH, Nickel MD, Peeters JM, Lee JM. Rapid imaging: recent advances in abdominal MRI for reducing acquisition time and its clinical applications. Korean J Radiol 2019;20:1597-1615.
7. Feinberg DA, Moeller S, Smith SM, et al. Multiplexed echo planar imaging for sub-second whole brain FMRI and fast diffusion imaging. PLoS One 2010;5:e15710.
8. Lau AZ, Tunnicliffe EM, Frost R, Koopmans PJ, Tyler DJ, Robson MD. Accelerated human cardiac diffusion tensor imaging using simultaneous multislice imaging. Magn Reson Med 2015;73:995-1004.
9. Morita K, Yoneyama M, Hamano H, et al. Multiband-SENSE EPI with variable-rate selective excitation (VERSE) pulses for accelerating abdominal DWI with respiratory triggering. 2021 International Society for Magnetic Resonance in Medicine (ISMRM) & Society for MR Radiographers & Technologists (SMRT) Annual Meeting & Exhibition; 2021 May 15-20; Vancouver, Canada. Concord, CA: ISMRM; 2021. program number.2133.
10. Lee D, Lustig M, Grissom WA, Pauly JM. Time-optimal design for multidimensional and parallel transmit variable-rate selective excitation. Magn Reson Med 2009;61:1471-1479.
11. Conolly S, Nishimura D, Macovski A, Glover G. Variable-rate selective excitation. J Magn Reson 1988;78:440-458.
12. Busse R, Li B, Li X. Improved slice profile and reduced fast spin echo spacing with variable-rate selective excitation. 11th Annual Meeting of International Society for Magnetic Resonance in Medicine (ISMRM); 2003 Jul 10-16; Toronto, Canada. Concord, CA: ISMRM; 2003. program number.956.
13. Zur Y, Hugg J, Montag A, Outmezguine D, Busse R. Clinical 3T SAR reduction using VERSE pulses. The 11th Annual Meeting of International Society for Magnetic Resonance in Medicine (ISMRM); 2003 Jul 10-16; Toronto, Canada. Concord, CA: ISMRM; 2003. program number.958.
14. Hirokawa Y, Isoda H, Maetani YS, et al. Hepatic lesions: improved image quality and detection with the periodically rotated overlapping parallel lines with enhanced reconstruction technique--evaluation of SPIO-enhanced T2-weighted MR images. Radiology 2009;251:388-397.
15. Boss A, Barth B, Filli L, et al. Simultaneous multi-slice echo planar diffusion weighted imaging of the liver and the pancreas: optimization of signal-to-noise ratio and acquisition time and application to intravoxel incoherent motion analysis. Eur J Radiol 2016;85:1948-1955.
16. Zhuo J, Gullapalli RP. AAPM/RSNA physics tutorial for residents: MR artifacts, safety, and quality control. Radiographics 2006;26: 275-297.
17. American College of Radiology. Liver imaging reporting and data system version 2018. Reston: American College of Radiology, 2018.
18. Yoon JK, Kim MJ, Lee S. Compressed sensing and parallel imaging for double hepatic arterial phase acquisition in gadoxetate-enhanced dynamic liver magnetic resonance imaging. Invest Radiol 2019;54:374-382.
19. Kim YY, Kim MJ, Gho SM, Seo N. Comparison of multiplexed sensitivity encoding and single-shot echo-planar imaging for diffusion-weighted imaging of the liver. Eur J Radiol 2020;132:109292.
20. Chakraborty DP. Recent advances in observer performance methodology: jackknife free-response ROC (JAFROC). Radiat Prot Dosimetry 2005;114:26-31.
21. Zheng B, Chakraborty DP, Rockette HE, Maitz GS, Gur D. A comparison of two data analyses from two observer performance studies using jackknife ROC and JAFROC. Med Phys 2005;32: 1031-1034.
22. Mandrekar JN. Measures of interrater agreement. J Thorac Oncol 2011;6:6-7.
23. Landis JR, Koch GG. The measurement of observer agreement for categorical data. Biometrics 1977;33:159-174.
24. Obele CC, Glielmi C, Ream J, et al. Simultaneous multislice accelerated free-breathing diffusion-weighted imaging of the liver at 3T. Abdom Imaging 2015;40:2323-2330.
25. Ciritsis A, Rossi C, Marcon M, Van VDP, Boss A. Accelerated diffusion-weighted imaging for lymph node assessment in the pelvis applying simultaneous multislice acquisition: a healthy volunteer study. Medicine (Baltimore) 2018;97:e11745.
26. Taron J, Martirosian P, Erb M, et al. Simultaneous multislice diffusion-weighted MRI of the liver: analysis of different breathing schemes in comparison to standard sequences. J Magn Reson Imaging 2016;44:865-879.
27. Jang W, Song JS, Kwak HS, Hwang SB, Paek MY. Intra-individual comparison of conventional and simultaneous multislice-accelerated diffusion-weighted imaging in upper abdominal solid organs: value of ADC normalization using the spleen as a reference organ. Abdom Radiol (NY) 2019;44:1808-1815.
28. Dietrich O, Heiland S, Sartor K. Noise correction for the exact determination of apparent diffusion coefficients at low SNR. Magn

Reson Med 2001;45:448-453.
29. Ohno N, Yoshida K, Ueda Y, et al. Diffusion-weighted imaging of the abdomen during a single breath-hold using simultaneous-multislice echo-planar imaging. Magn Reson Med Sci 2023;22:253-262.
30. Taron J, Martirosian P, Schwenzer NF, et al. Scan time minimization in hepatic diffusion-weighted imaging: evaluation of the simultaneous multislice acceleration technique with different acceleration factors and gradient preparation schemes. MAGMA 2016;29:739-749.
31. Taron J, Martirosian P, Kuestner T, et al. Scan time reduction in diffusion-weighted imaging of the pancreas using a simultaneous multislice technique with different acceleration factors: how fast can we go? Eur Radiol 2018;28:1504-1511.